Electronic and optical properties of red HgI_2

R. Ahuja, O. Eriksson, and Börje Johansson
Condensed Matter Theory Group, Department of Physics, Uppsala University, Box 530 S-751 21, Uppsala, Sweden

S. Auluck
Department of Physics, University of Roorkee, Roorkee-247 667, India

J. M. Wills
Theoretical Division, Los Alamos National Laboratory, Los Alamos, New Mexico 87544
(Received 29 February 1996; revised manuscript received 5 June 1996)

Within the local-density approximation we have used the linear muffin-tin orbital method, without geometrical approximations, to calculate the electronic structure of red HgI_2. Using the self-consistent potential we have calculated the energy bands and from these derived the anisotropic frequency-dependent dielectric function and the reflectivity spectrum. The calculated dielectric function is in good agreement with the experimental data in contrast to previous theoretical work. The effect of the spin-orbit coupling on the optical properties has also been studied and found to be significant. In this work we predict a rather large anisotropy in the dielectric function resulting from the low-symmetry crystal structure. [S0163-1829(96)06539-3]

I. INTRODUCTION

There has been a renewed interest in mercuric iodide (HgI_2) in order to obtain further knowledge about its structural and physical properties. HgI_2 crystallizes in a tetragonal structure[1] at low temperatures and has a measured band gap of 2.13 eV at 30 °C and a red appearance.[2] It undergoes a crystalline transformation at 127 °C to an orthorhombic structure which remains stable up to the melting point of 259 °C. The yellow color of this high temperature orthorhombic phase suggests a decrease of the band gap by about 10%. As a result of the relatively large atomic masses of the constituent elements ($Z=80$ for Hg and $Z=53$ for I), HgI_2 has a stopping power for photons. Its high bulk electrical resistivity[3] ensures a low dark current during detector operation and a high photosensitivity so that the number of generated electron-hole pairs is proportional to the incident photon energy. This makes HgI_2 well suited as a detector material for x-ray and γ-ray spectroscopies.[4] Besides these useful properties there are, however, also some disadvantages with HgI_2, such as the problems associated with the small hole mobility (at room temperature and along the c axis)[5] and the fact that HgI_2 has a high vapor pressure, which means that the crystal should not be exposed to vacuum during measurements.

Although not too many detailed experiments have been reported on this material, a number of articles dealing with optical properties have been published. Novikov and Pimonenko[6] have investigated the exciton absorption and luminesence of HgI_2 at low temperatures. They have also determined the temperature dependence of the absorption and photoluminescence. Kanzaki and Imai[7] have measured the optical spectra of tetragonal HgI_2 in the 2–6 eV photon energy region. They described the main part of the dichroic optical spectra by optical transitions from three p-like valence bands. Moreover, Anedda *et al.*[8] have made a detailed study of excitons in red HgI_2 by means of wavelength-modulated reflectivity (WMR) experiments at 2 K. They have shown that the excitonic spectrum has a strong ground-state anomaly. Lately Anedda *et al.*[9] have also studied the reflectivity in the spectral range of 2–10 eV at 100 K and the optical constants were deduced by means of the Kramers-Kronig relations. Sakuma *et al.*[10] have also studied the optical spectrum by means of WMR and magnetic circular dichroism. They have observed many fine structures in the spectrum and assigned them as due to the so-called phonon replicas of the $2s$ exciton. Bloch *et al.*[11] have observed the cyclotron resonance of electrons and holes below 4.2 K using a cross modulation technique at a microwave frequency of 137 GHz and suggested a reinterpretation of the experimental exciton spectra. Very recently Gonzalez and Ibarra[12] have measured the effect of small deformations on the optical properties of HgI_2. They found that the gap position decreases slightly with pressure.

The electronic structure of this material has also been investigated theoretically. For instance, there have been three recent energy band structure calculations on HgI_2.[13–15] Yee, Sherohman, and Armentout[13] were the first to report such calculations. They employed the empirical pseudopotential method. However, the calculations were done for an incorrect (BCT) crystal structure. Moreover, these calculations were nonrelativistic and non-self-consistent. More recently Chang and James[15] have improved upon the calculation of Yee *et al.*[13] by using an empirical nonlocal pseudopotential, where the calculated energy gap has been adjusted to the experimental value. In this work, the spin-orbit interaction was included using first order, degenerate perturbation theory. Chang and James also derived the electron and hole effective masses and the complex dielectric function. However, also these calculations were not self-consistent. The only self-consistent calculation has been performed by Turner and Harmon[14] (TH), who used the Korringa-Kohn-Rostoker (KKR) method. For the relativistic calculations (i.e., including the spin-orbit coupling) the linear augmented

plane wave (LAPW) method was used. Both these calculations used a muffin-tin approximation of the potential. A comparison between the theoretical papers shows that the band structures of Chang and James[15] and Turner and Harmon[14] are actually quite similar. The calculation by Turner and Harmon gives a band gap of 0.5 eV [this deviation from experiment is expected in local-density approximation (LDA) calculations, which are known to underestimate band gaps by as much as 50%], whereas in the calculations by Chang and James the band gap is adjusted to the experimental value (2.13 eV). The calculations in Refs. 14 and 15 give electron and/or hole masses that are in agreement with each other and with the experimental data. In the work by Turner and Harmon the ionicity was also investigated as well as the chemical bonding.

Earlier interest in the optical properties of HgI_2 has primarily been to understand the hydrogenlike exciton series ($n=1,2$ states) near the fundamental edge, which manifests itself in the absorption, reflectivity, photoconductivity, and luminescence. Although there have been numerous studies of the interaction of light with HgI_2, the frequency-dependent dielectric function has not been given very much attention for this material. The only published calculation of the frequency-dependent complex dielectric function, $\epsilon(\omega)$, has been done using a non-self-consistent method.[15] In this latter study, by introducing empirical parameters, it was claimed that good agreement with recent data for $\epsilon(\omega)$ was achieved. However, the agreement between experiment and theory is not as good as we have found in more accurate calculations of $\epsilon(\omega)$ for other materials. Since the crystal structure of HgI_2 is open and the calculated properties rely on accurate eigenvalues and eigenvector, it is most probably important to calculate the electronic structure of HgI_2 using a full-potential method, in order to give accurate theoretical dielectric functions. To our knowledge no such *ab initio* calculations have been published before. Moreover, it seems that there is a lack of both experimental as well as theoretical data on the anisotropic optical properties of HgI_2. Since the material is tetragonal with a rather large c/a ratio one may expect such an anisotropy. These observations have motivated us to compute $\epsilon(\omega)$ using a self-consistent calculation based on a full-potential method and we report on such a study in the present paper. We have done this in order to give the best possible parameter-free theoretical optical data of HgI_2.

II. DETAILS OF CALCULATIONS

In order to study the electronic structure of HgI_2 we have used the full-potential linear muffin-tin orbital (FPLMTO) method.[16] The calculations were based on the local-density approximation with the Hedin-Lundqvist[17] parametrization for the exchange and correlation potential. The spin-orbit coupling was included explicitly. Basis functions, electron densities, and potentials were calculated without any geometrical approximation.[16] These quantities were expanded in combinations of spherical harmonic functions (with a cutoff $\ell_{max}=8$) inside nonoverlapping spheres surrounding the atomic sites (muffin-tin spheres) and in a Fourier series in the interstitial region. The muffin-tin spheres occupied approximately 50% of the unit cell. The radial basis functions within the muffin-tin spheres are linear combinations of radial wave functions and their energy derivatives, computed at energies appropriate to their site and principal as well as orbital atomic quantum numbers, whereas outside the muffin-tin spheres the basis functions are combinations of Neuman or Hankel functions.[18,19] In the calculations reported here, we made use of pseudocore $5p$ states for Hg and pseudocore $4d$ states for I, and valence band $6s$, $6p$, and $5d$ basis functions for Hg and $5s$ and $5p$ basis functions for I with two corresponding sets of energy parameters, one appropriate for the semicore $5p$ and $4d$ states and the other appropriate for the valence states. The resulting basis formed a single, fully hybridizing basis set. This approach has previously proven to give a well converged basis.[16] For sampling the irreducible wedge of the Brillouin-zone we used the special k-point method.[20] In order to speed up the convergence we have associated each calculated eigenvalue with a Gaussian broadening of width 10 mRy.

The crystal structure of HgI_2 is simple tetragonal with $a=4.361$ Å and $c=12.450$ Å. The positions of the two Hg atoms are at (0,0,0; 0.5,0.5,0.5) and the four I atoms are at ($0.0,0.5,u$; $0.5,0.0,-u$; $0.0,0.5,u+0.5$, and $0.5,0.0,0.5-u$) with $u=0.14$. Since c/a is large, the structure is fairly open. This circumstance suggests that a full-potential method is needed in order to achieve an adequate theoretical description of the basic electronic structure of the present compound.

Calculation of the dielectric function

The ($q=0$) dielectric function was calculated in the momentum representation, which requires matrix elements of the momentum, $\mathbf{p}$, between occupied and unoccupied eigenstates. To be specific, the imaginary part of the dielectric function, $\epsilon_2(\omega)\equiv \mathrm{Im}\epsilon(\mathbf{q}=0,\omega)$, was calculated from[21]

$$\epsilon_2^{ij}(\omega)=\frac{4\pi^2e^2}{\Omega m^2\omega^2}\sum_{\mathbf{k}nn'\sigma}\langle \mathbf{k}n\sigma|p_i|\mathbf{k}n'\sigma\rangle\langle \mathbf{k}n'\sigma|p_j|\mathbf{k}n\sigma\rangle \times f_{\mathbf{k}n}(1-f_{\mathbf{k}n'})\,\delta(e_{\mathbf{k}n'}-e_{\mathbf{k}n}-\hbar\omega). \quad (1)$$

In Eq. (1), e is the electron charge, m its mass, Ω is the crystal volume, and $f_{\mathbf{k}n}$ is the Fermi distribution. Moreover, $|\mathbf{k}n\sigma\rangle$ is the crystal wave function corresponding to the nth eigenvalue with crystal momentum $\mathbf{k}$ and spin σ. With our spherical wave basis functions, the matrix elements of the momentum operator are conveniently calculated in spherical coordinates and for this reason the momentum is written $\mathbf{p}=\Sigma_\mu \mathbf{e}_\mu^* p_\mu$,[22] where μ is -1, 0, or 1, and $p_{-1}=1/\sqrt{2}(p_x-ip_y)$, $p_0=p_z$, and $p_1=-1/\sqrt{2}(p_x+ip_y)$.[23]

The evaluation of the matrix elements in Eq. (1) is done over the muffin-tin region and the interstitial separately. The integration over the muffin-tin spheres is done in a way similar to what Oppener[24] and Gasche[21] did in their calculations using the atomic sphere approximation (ASA). A full detailed description of the calculation of the matrix elements will be presented elsewhere.[25]

The summation over the Brillouin zone in Eq. (1) is calculated using linear interpolation on a mesh of uniformly distributed points, i.e., the tetrahedron method. Matrix elements, eigenvalues, and eigenvectors are calculated in the

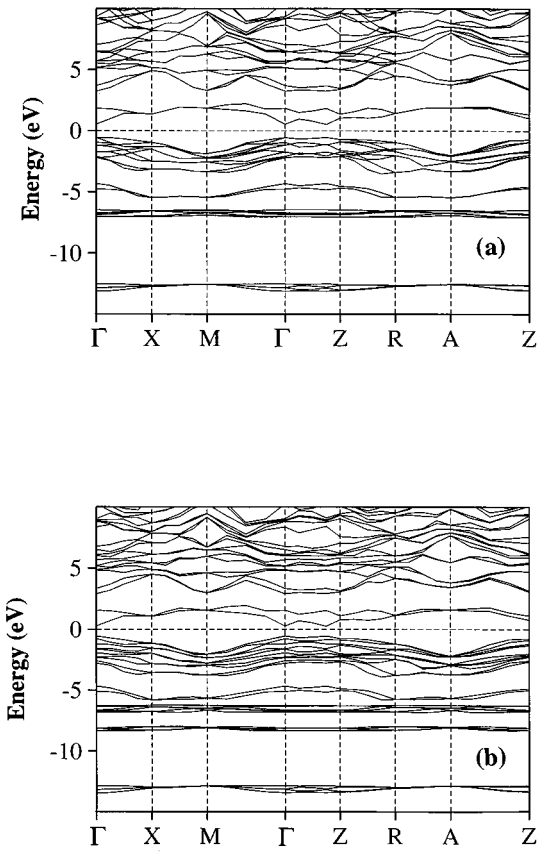

FIG. 1. Calculated energy band structure of HgI_2, (a) neglecting the spin-orbit coupling (SO), (b) including the spin-orbit coupling (SO), along the major symmetry directions. The Fermi level (E_F) is set at zero energy.

irreducible part of the Brillouin-zone. The correct symmetry for the dielectric constant was obtained by averaging the calculated dielectric function. Finally, the real part of the dielectric function, $\epsilon_1(\omega)$, is obtained from $\epsilon_2(\omega)$ using the Kramers-Kronig transformation,

$$\epsilon_1(\omega) \equiv \mathrm{Re}(\epsilon(\mathbf{q}=0,\omega)) = 1+\frac{1}{\pi}\int_0^\infty d\omega'\,\epsilon_2(\omega')\left(\frac{1}{\omega'-\omega}+\frac{1}{\omega'+\omega}\right). \quad (2)$$

For a tetragonal or hexagonal structure we need to calculate two components of the total dielectric function, corresponding to light polarized parallel and perpendicular to the c axis. In that case the total, orientation averaged ϵ_2 is given by

$$\epsilon_2^{tot}(\omega)=\frac{\epsilon_2^{\parallel}(\omega)+2\,\epsilon_2^{\perp}(\omega)}{3}. \quad (3)$$

III. RESULTS AND DISCUSSIONS

A. Band structure and density of states

Since the optical spectra are calculated from interband transitions, we find it of interest to first describe our calculated electronic structure. For this reason we show the calculated energy band structure for HgI_2 in Fig. 1. At the top of the figure [Fig. 1(a)] we show the energy bands obtained when the spin-orbit coupling is not included in the theoretical treatment and in the lower part [Fig. 1(b)] the results when the spin-orbit coupling is included. To a large extent the two band structures look essentially the same except that some of the bands in the lower part of the figure are split due to the spin-orbit coupling. In HgI_2, there are four energetically low-lying bands, which are derived from the $5s$ states of the iodine and these bands are positioned around -13.0 eV below the Fermi energy. For a somewhat lower binding energy there are ten Hg $5d$ bands which are centered around -7.0 eV in Fig. 1(a). In Fig. 1(b) these ten Hg $5d$ bands are split due to the spin-orbit coupling which is about 2.1 eV. In Fig. 1(b) these bands are positioned between -8.2 and -6.1 eV. The next two bands around -5.0 eV are derived from the Hg $6s$ and the bonding I $5p_z$ states. After this the next ten bands originate from the I $5p$ states and they are positioned between -2.2 and -0.55 eV. As can be seen in Fig. 1(a), the two top bands in this group are degenerate at the Γ point, but in Fig. 1(b) these two top bands are split due to the spin-orbit coupling. The next two bands are a mixture of states derived from the Hg $6s$ and the I $5p_z$ states. These bands are just above the band gap. Overall our band structure is quite similar to those reported in Refs. 14 and 15, although the magnitudes of the band gaps in the different calculations differ somewhat.

Our calculated direct energy band gap is 1.1 eV and is located at the zone center. When the spin-orbit coupling is included the band gap is reduced and becomes 0.82 eV. Thus our calculated band gap is considerably smaller than the experimental value of 2.13 eV at 30 °C.[2] Turner and Harmon[14] obtained a somewhat lower band gap (0.52 eV) when the spin-orbit coupling was included. This difference may be due to the muffin-tin approximation which is used by Turner and Harmon, whereas we are using a general potential. It is well known that LDA in general underestimates energy band gaps. Thus to get the correct value of the gap one will need to include correlations similar to those used for Si (Ref. 26) and NiO.[27]

The calculated density of states (DOS) is shown in Fig. 2(a) and Fig. 2(b), without and with spin-orbit coupling, respectively. The major contributions to the occupied part of the DOS come from the Hg d and Hg s states and the I s and I p states. The total DOS has many structures: (a) a peak around -14.0 eV arising from the I s states; (b) a narrow structure around -7.5 eV arising form the Hg d states; (c) a structure around -6.0 eV from the I p_z and Hg s states; (d) a broad structure between -4.2 and -1.1 eV from the I p states; and (e) a structure just after the band gap arising from the I-p_z and Hg-s states. With the spin-orbit coupling included in the calculations, [Fig. 2(b)] the Hg $5d$ states are split by about 2.1 eV, which is close to the atomic value. Turner and Harmon have calculated this splitting to be 1.8 eV. The narrowness of the Hg $5d$ states reflects their core-like nature. Our calculated DOS is by and large in good agreement with the calculation of Turner and Harmon.

A first reaction to the information given in Figs. 1 and 2 is that the inclusion of the spin-orbit coupling has only marginal effects on the electronic structure except for the Hg d states. The DOS curves are for instance quite similar in Fig. 2(a) and Fig. 2(b). The reason for this is that the dispersion of the Hg and I p states is larger than the spin-orbit splitting.

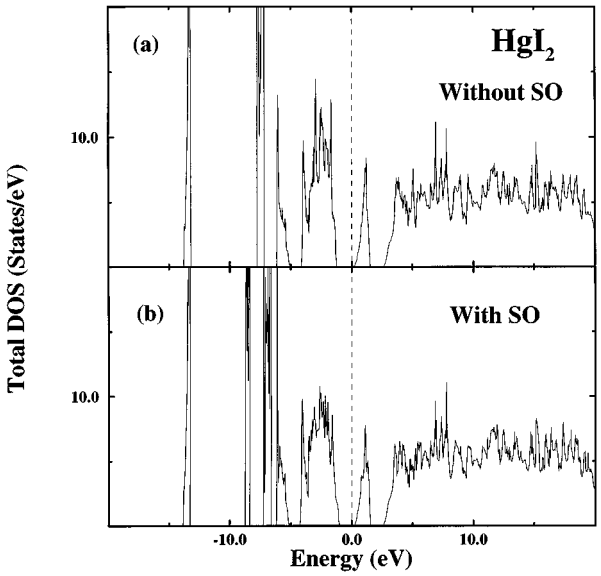

FIG. 2. Calculated total density of states (DOS) for HgI_2. In (a) the spin-orbit coupling (SO) is neglected, while in (b) it is included. The Fermi level is set at zero energy and marked by a vertical dotted line.

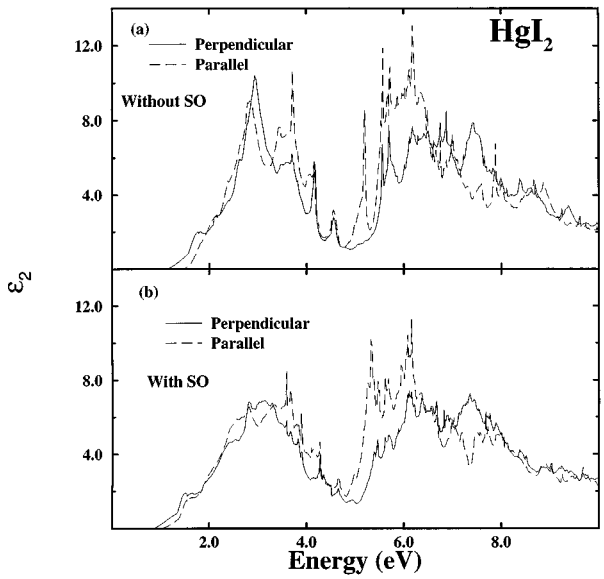

FIG. 4. The calculated ϵ_2 for HgI_2 (a) without and (b) with the spin-orbit coupling. ''Parallel'' refers to the electric field parallel to the c axis and ''Perpendicular'' refers to the electric field perpendicular to the c axis.

However, as we will demonstrate below, the calculated optical spectra are more affected by the spin-orbit coupling. This is due to the fact that the wave function character is more influenced by the spin-orbit coupling than the one particle energy dispersion.

B. Optical properties

There is only one experimental paper[9] which reports on the frequency-dependent reflectivity and the imaginary part of the dielectric function. Therefore in the present work we will mainly discuss these two properties. Unfortunately it was not stated in Ref. 9 whether in the experiments the electric field vector was parallel or perpendicular to the crystallographic c axis. For this reason we will compare the theoretical ϵ_2^{tot} [Eq. (3)] with the experimental data. In Fig. 3 we show our calculated imaginary part of ϵ_2^{tot} (with the spin-orbit coupling included in the calculation) together with experimental data. The calculated ϵ_2^{tot} is broadened with a Gaussian function with a width at half maximum of 0.02 eV. The calculated ϵ_2^{tot} shows two major structures, one at around 3.0 eV and a broad structure between 5.5 to 7.5 eV. In the experimental data the corresponding structures are positioned around 4.0 and 6.5 eV, respectively. The difference in peak positions is due to the fact that our calculated band gap is smaller than the experimental gap by 1.0 eV. The calculated height of the first structure is smaller than the experimental data and the height of the second structure is a little bit larger than the experiment. Still, by and large, the calculated imaginary part of ϵ_2^{tot} is in rather good agreement with the data when a shift of the band gap is taken into account. On the other hand, if we compare our calculated ϵ_2 with previous calculations by Chang and James we note a rather large disagreement.

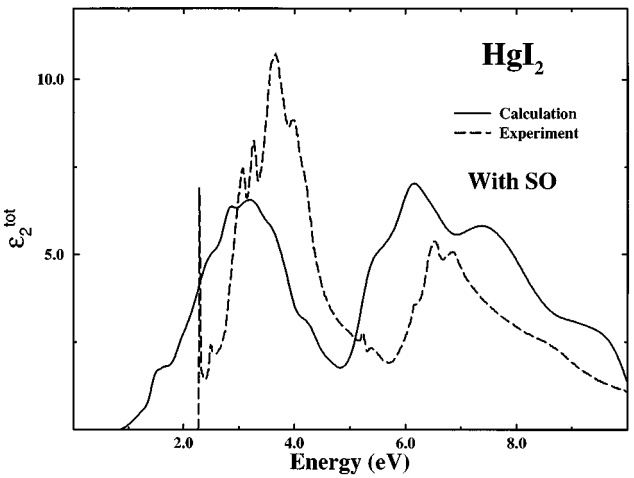

FIG. 3. The calculated (solid line) ϵ_2^{tot} (including the spin-orbit coupling) along with the experimental (Ref. 9) (dashed line) for HgI_2.

Figure 4 shows the calculated results for ϵ_2 (without broadening) both for the electric field vector parallel and perpendicular to the crystallographic c axis. In this figure we also compare optical spectra when the spin-orbit coupling is omitted and included. A number of things may be deduced from Fig. 4. First of all, we note that although the calculated electronic structure is rather insensitive to whether or not the spin-orbit coupling is included, the calculated optical spectra do show sensitivity to this interaction. This is clear from certain peaks in Fig. 4(a) where for $\epsilon_2^{\parallel}$ there is a sharp peak at $\sim$5.2 eV, which is absent in Fig. 4(b). Figure 4(a) also shows a two peak feature at 2.8 and 3.8 eV for $\epsilon_2^{\parallel}$, which in Fig. 4(b) is found only as a broad feature in this energy range. Thus it is clear that the inclusion of spin-orbit coupling influences the optical spectra to a larger degree compared to the eigenvalues. Clearly the spin-orbit coupling in-

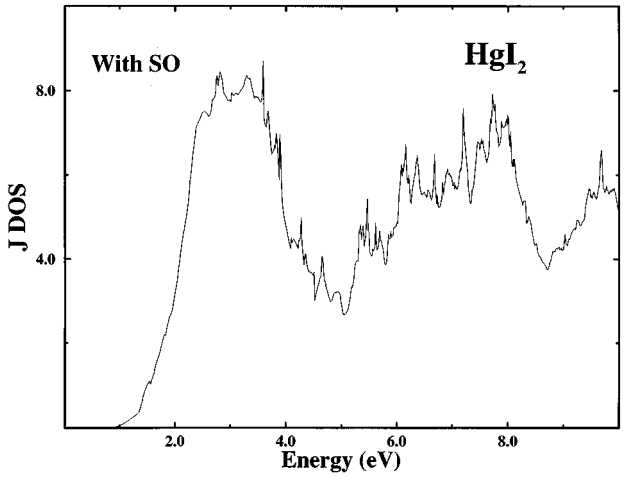

FIG. 5. The joint density of states (JDOS) of HgI_2 (including the spin-orbit coupling).

fluences the wave function character of the different one-electron levels and through this also the optical matrix elements in Eq. (1).

Figure 4 also shows that $\epsilon_2^{\parallel}$ and $\epsilon_2^{\perp}$ are quite different. This anisotropy in the optical properties is typical for low-symmetry crystals. Since the experimental data did not distinguish between the parallel and perpendicular components of the polarization of the light, we hope our theoretical prediction of the anisotropic optical properties in HgI_2 will stimulate further experimental work. The real part of the dielectric constant is enhanced near the fundamental gap in comparison to the experiment. Without the spin-orbit coupling, we get $\epsilon_1^{\perp} \approx 6.6$ and $\epsilon_1^{\parallel} \approx 6.9$ near the band gap (figure not shown), whereas the experimental values are $\epsilon_1^{\perp} \approx 5.15$ and $\epsilon_1^{\parallel} \approx 6.8$.[11] With the spin-orbit coupling included, the dielectric constant has a slightly larger value than without the spin-orbit coupling; $\epsilon_1^{\perp}$ is ≈ 6.7 and $\epsilon_1^{\parallel}$ is ≈ 7.0 whereas Chang and James have reported 5.4 and 5.8, respectively. Therefore we conclude that the calculated dielectric constant shows a somewhat smaller anisotropy than observed experimentally. Our calculated ϵ_2 functions are quite different compared to the ones reported by Chang and James, and agree much better with the experimental data. This difference illustrates that a theoretical description of the dielectric response depends on the accuracy of the method.

In order to analyze our calculated ϵ_2^{tot} curves we have also calculated the joint density of states (JDOS), i.e., when setting all matrix elements equal to unity. Note that the JDOS curve (Fig. 5) is somewhat similar to the calculated ϵ_2^{tot} in Fig. 3. The first structure has higher intensity than the second structure but the inclusion of the matrix elements reduces the intensity of the first structure somewhat. However, when compared to $\epsilon_2^{\parallel}$ and $\epsilon_2^{\perp}$ in Fig. 4 we note that the inclusion of matrix elements is important giving the above described anisotropy in the optical properties. We conclude that approximating the optical response of a material by the JDOS, an approximation quite frequently used, is not a good approximation.

In Figs. 6(a) and 6(b) we show the reflectivity spectrum of HgI_2 corresponding to $E_{\perp}$ and $E_{\parallel}$ polarization. The calculations have been performed both without and with the spin-

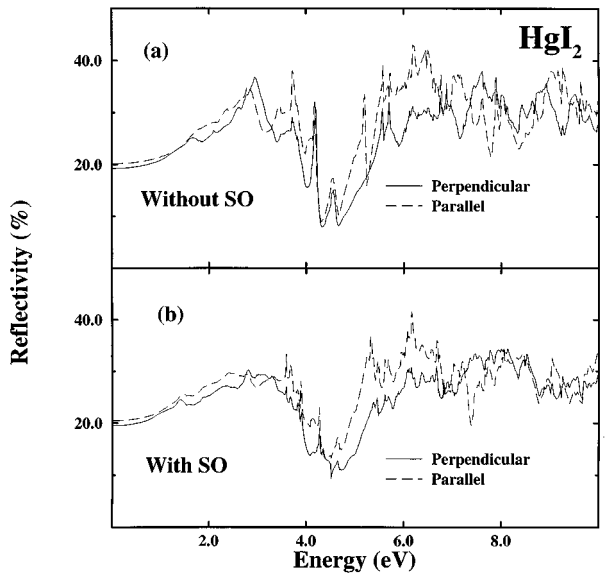

FIG. 6. The calculated reflectivity for HgI_2 (a) without and (b) with the spin-orbit coupling.

orbit (SO) coupling. The experimental reflectivity spectrum of HgI_2 by Anedda *et al.*[9] is compared to our theoretical data in Fig. 7. Our calculated reflectivity starts at around a 20% reflectivity, irrespective of whether the spin-orbit coupling is included or not, which is in good agreement with the experimental value. Our reflectivity reaches a maximum value of around 30% at 3.0 eV, whereas the experimental reflectivity is a little higher at this energy. The dip in the calculated reflectivity is found at around 4.5 eV whereas experimentally the dip is at around 5.5 eV. The value of the reflectivity is 10% at the dip and this is quite similar to the experimental value. After the dip the reflectivity increases, and reaches again the value of 30% and then it decreases slightly. Our calculated spectrum without SO shows that the first and second structures have almost the same reflectivity, but with SO included the first structure has a somewhat smaller reflectiv-

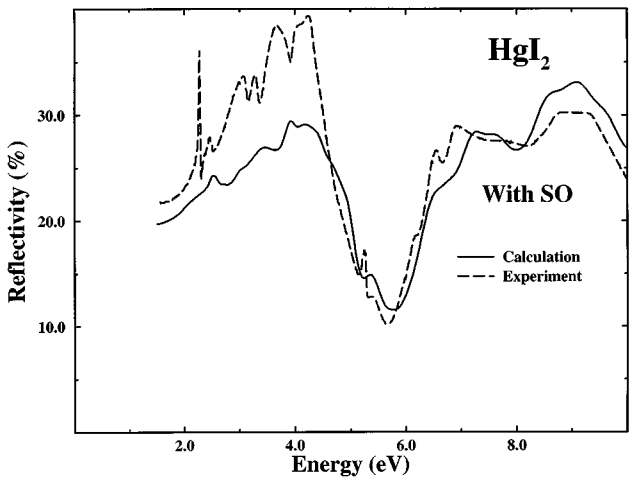

FIG. 7. The broadened calculated (solid line) reflectivity ($\perp$) with the spin-orbit coupling along with the experimental (Ref. 9) (dashed line) for HgI_2. The calculated curve is shifted 1.3 eV towards higher energy to match the experimental band gap.

ity than the second structure. When comparing calculations with and without spin-orbit coupling we note that details in the reflectivity are sensitive to the inclusion of relativistic effects. Thus, we again come to the conclusion that it is necessary to include spin-orbit coupling to get a good description of the optical properties of HgI_2. The experiments show that the first structure has a larger reflectivity than the second structure. This difference in the reflectivity is not found in the theoretical curve (Fig. 7). The agreement between experiment and theory is therefore not perfect although the overall shape of the two curves in Fig. 7 is the same.

IV. CONCLUSIONS

We have studied the electronic and optical properties of HgI_2 using the FPLMTO method with and without spin-orbit coupling. The inclusion of the spin-orbit coupling reduces the band gap by about 0.30 eV. The spin-orbit coupling also has a rather large effect on the details of the peak positions and peak intensities of the calculated spectrum of the dielectric function and the reflectivity. Our calculated real part of the dielectric function near the fundmental gap is in good agreement with experiment for $E_{\parallel}$ polarization, while for $E_{\perp}$ polarization it is a little bit too large. For the imaginary part of the dielectric function, as well as for the reflectivity, our calculations reproduce experiments rather well. This is in contrast to previous empirical work where the agreement was not good. Clearly an accurate theoretical method is needed for reproducing optical data and this is especially critical for more open structures, such as the structure studied here. Finally we have made a prediction that there is rather large anisotropy in the optical properties of HgI_2 and we hope our work will stimulate further experimental activities.

ACKNOWLEDGMENTS

We wish to thank the Swedish Natural Research Council and the Swedish Materials Consortium No. 9 financed by NUTEK and NFR for valuable support. One of us (S.A.) would like to thank the Swedish Institute for financial support and the Condensed Matter Theory Group at Uppsala University for their kind hospitality. Part of these calculations was done at the Swedish Supercomputer Centre in Linköping, Sweden.

[1] R.W.G. Wyckoff, *Crystal Structures*, 2nd ed. (Interscience, New York, 1963), Vol. 1, p. 309.

[2] An extensive review of the physical properties of α-HgI_2 is contained in a report by M. Piechotka and E. Kaldis, Laboratorium für Festkörperphysik, Eidgenössiche Technische Hochschule-Zürich, Report No. CH-8093, Zürich, 1984 (unpublished).

[3] H.L. Malm, T.W. Raudoff, M. Martina, and K.R. Zanio, IEEE Trans. Nucl. Sci. **NS-20**, 500 (1973).

[4] See, for example, the review by R.C. Whited and M. Schieber, Nucl. Instrum. Methods **162**, 119 (1979).

[5] G. Ottaviani, C. Canali, and A. Alberigi Quaranta, IEEE Trans. Nucl. Sci. **NS-22**, 192 (1975); R. Minder, G. Ottaviani, and C. Canali, J. Phys. Chem. Solids **37**, 417 (1976).

[6] B.V. Novikov and N.M. Pimonenko, Fiz. Tekh. Poluprovodn. **4**, 2077 (1970) [Sov. Phys. Semicond. **4**, 1785 (1970)].

[7] K. Kanzaki and I. Imai, J. Phys. Soc. Jpn. **32**, 1003 (1972).

[8] A. Anedda, F. Raga, E. Grilli, and M. Guzzi, Nuovo Cimento **38**, 439 (1977).

[9] A. Anedda, E. Grilli, M. Guzzi, F. Raga, and A. Serpi, Solid State Commun. **39**, 1121 (1981).

[10] F. Sakuma, H. Fukutani, and G. Kuwabara, Phys. Soc. Jpn. **45**, 1349 (1978).

[11] P.D. Bloch, J.W. Hodby, C. Schwab, and D.W. Stacey, J. Phys. C **11**, 2579 (1978).

[12] M. González and A. Ibarra, Phys. Rev. B **51**, 13 786 (1995).

[13] J.H. Yee, J.W. Sherohman, and G.A. Armantrout, IEEE Trans. Nucl. Sci. **NS-23**, 117 (1976).

[14] D.E. Turner and B.N. Harmon, Phys. Rev. B **40**, 10 516 (1989).

[15] Y.C. Chang and R.B. James, Phys. Rev. B **46**, 15 040 (1992).

[16] J. M. Wills, (unpublished); J.M. Wills and B.R. Cooper, Phys. Rev. B **36**, 3809 (1987); D.L. Price and B.R. Cooper, *ibid.* **39**, 4945 (1989)

[17] L. Hedin and B.I. Lundqvist, J. Phys. C **4**, 2064 (1971).

[18] O. K. Andersen , Phys. Rev. B **12**, 3060 (1975).

[19] H. L. Skriver, *The LMTO Method* (Springer, Berlin, 1984).

[20] D.J. Chadi and M.L. Cohen, Phys. Rev. B **8**, 5747 (1973); S. Froyen, *ibid.* **39**, 3168 (1989)

[21] C.S. Wang and J. Callaway, Phys. Rev. B **9**, 4897 (1974); a good description of the calculation of dielectric constants and related properties is found in the thesis by T. Gashe, Uppsala University, 1993.

[22] A. R. Edmonds, *Angular Momentum in Quantum Mechanics* (Princeton University Press, Princeton, 1974), p. 82.

[23] In practice we calculate matrix elements of the symmetrized momentum operator $\langle i|\vec{p}_{\mu}|j\rangle \equiv [\langle i|p_{\mu}j\rangle + (-1)^{\mu}\langle p_{-\mu}i|j\rangle]/2$.

[24] P.M. Oppeneer, T. Maurer, J. Sticht and J. Kübler, Phys. Rev. B **45**, 10 924 (1992).

[25] R. Ahuja, S. Auluck, J.M. Wills, M. Alouani, B. Johansson, and O. Eriksson (unpublished).

[26] C.S. Wang and W.E. Pickett, Phys. Rev. Lett. **51**, 597 (1983).

[27] B.H. Brandow, Adv. Phys. **26**, 651 (1977); V.I. Anisimov, I.V. Solovyev, M.A. Korotin, M.T. Czyzyk, and G.A. Sawatsky, Phys. Rev. B **48**, 16 929 (1993).